

Does Bimolecular Charge Recombination in Highly Exergonic Electron Transfer Afford the Triplet Excited State or the Ground State of a Photosensitizer?

Motonobu Murakami,[†] Kei Ohkubo,[†] Paulami Mandal,[‡] Tapan Ganguly,[‡] and Shunichi Fukuzumi^{*,†}

Department of Material and Life Science, Graduate School of Engineering, Osaka University, SORST, Japan Science and Technology Agency (JST), Suita, Osaka 565-0871, Japan, and Department of Spectroscopy, Indian Association for the Cultivation of Science, Jadavpur, Kolkata 700 032, West Bengal, India

Received: August 23, 2007; In Final Form: October 15, 2007

The investigations were made on photoinduced electron transfer (ET) from the singlet excited state of rubrene (¹RU*) to *p*-benzoquinone derivatives (duroquinone, 2,5-dimethyl-*p*-benzoquinone, *p*-benzoquinone, 2,5-dichloro-*p*-benzoquinone, and *p*-chloranil) in benzonitrile (PhCN) by using the steady state and time-resolved spectroscopies. The photoinduced ET produces solvent-separated type charge-separated (CS) species and the charge-recombination (CR) process between RU radical cation and semiquinone radical anions obeys second-order kinetics. Not only the CS species but also the triplet excited state of RU (³RU*) is seen in the transient absorption spectra upon laser excitation of a PhCN solution of RU and *p*-benzoquinone derivatives. The comparison of their time profiles clearly suggests that the CR process between RU radical cation and semiquinone radical anions to the ground state is independent from the deactivation of ³RU*. This indicates that the CR in a highly exergonic ET occurs at a longer distance with a large solvent reorganization energy, which results in faster ET to the ground state than to the triplet excited state that is lower in energy than the CS state. Photoinduced ET from ³RU* in addition from ¹RU* also occurs when *p*-benzoquinone derivatives with electron-withdrawing substituents were employed as electron acceptors.

Introduction

Photoinduced electron transfer (ET) between the excited state of sensitizer and the ground state substrate forms the radical ion pair and charge-separated species.^{1–17} This separation of charges between the electron donors and acceptors proceeds followed by energy wasting charge-recombination (CR) processes, which might occur by either first- or second-order or a combination of both processes depending upon the binding power of the radical ion-pair complex initially formed. It is known that the decay of the contact radical ion-pair (CRIP) obeys first-order kinetics when intramolecular ET in CRIP occurs in the solvent cage.^{1–6} On the other hand the decay of solvent-separated radical ion-pair (SSRIP) species obeys the diffusion-assisted second-order kinetics, when intermolecular ET of SSRIP species occurs.^{1–3,6,7a}

Because ET quenches the fluorescence from the excited states of photosensitizers, steady state fluorescence and time-resolved fluorescence measurements are the useful tools to investigate ET reactions of the excited state of photosensitizers.^{18–20} In bimolecular forward ET reactions, the ET rate constant generally increases with increasing the ET driving force ($-\Delta G_{\text{et}}$) up to a diffusion-limited value and remains unchanged even at the larger $-\Delta G_{\text{et}}$.^{6,7,18–20} Marcus theory of ET predicts the decrease in the ET rate constant in the region where the ET driving force is larger the reorganization energy of ET (λ), ($-\Delta G_{\text{et}} > \lambda$).^{21,22} This region is called the Marcus inverted region. The Marcus inverted region is commonly observed for in the intra- or

monomolecular systems.^{23–29} In contrast, the Marcus inverted region has scarcely been observed for bimolecular ET reactions.³⁰ A rare example of the observation of the Marcus inverted region for bimolecular ET reaction involves the one-electron oxidation or reduction of fullerenes which have small λ of ET.³¹

There are mainly two hypotheses to account for the lack of the observation of the Marcus inverted region.³² One is the case in which the CR primary product is the triplet excited state rather than the ground state of photosensitizers.³³ In this case, the actual driving force is no longer large and CR to the triplet excited state occurs in the Marcus normal region. The other hypothesis comes from the distance between radical ions, which may increase with increasing the driving force of CR.^{34,35} The longer distance for ET of SSRIP as compared with ET of CRIP results in the larger solvent λ , when it becomes more difficult to reach the Marcus inverted region ($-\Delta G_{\text{et}} > \lambda$).²⁰ These two hypotheses can be distinguished if one examines the dynamics of CR with the driving force that is larger than the triplet excited state energy of photosensitizers. If the CR affords the triplet excited state, the CR rate would coincide with the rate of formation of the triplet excited state. However, there has so far been no report on such distinction of the CR to the triplet vs ground state of photosensitizers.

We report herein the dynamics of photoinduced ET from the singlet excited state of rubrene (¹RU*) to *p*-benzoquinone derivatives (duroquinone (DQ), 2,5-dimethyl-*p*-benzoquinone (Me₂Q), *p*-benzoquinone (Q), 2,5-dichloro-*p*-benzoquinone (Cl₂Q), and *p*-chloranil (Cl₄Q) in Chart 1) to distinguish between the two CR pathways to the triplet and ground state of RU. RU is chosen as a photosensitizer because it has a low lying triplet excited state.³⁶ There have been many reports for development of long-lifetime, high-efficiency white organic light-emitting

* Corresponding author. Tel.: +81 6 6879 7368. Fax: +81 6 6879 7370. E-mail address: fukuzumi@chem.eng.osaka-u.ac.jp.

[†] Osaka University.

[‡] Indian Association for the Cultivation of Science.

diodes with rubrene.^{37–39} The investigations were made on photoinduced ET reactions between RU and *p*-benzoquinone derivatives in benzonitrile by using the steady state, time-resolved spectroscopic (fluorescence lifetimes and transient absorption measurements by the pump–probe technique) measurements.

Experimental Section

Materials. Rubrene (5,6,11,12-tetraphenyltetracene; RU), duroquinone (tetramethyl-*p*-benzoquinone; DQ), 2,5-dimethyl-*p*-benzoquinone (Me₂Q), *p*-benzoquinone (Q), 2,5-dichloro-*p*-benzoquinone (Cl₂Q), and *p*-chloranil (tetrachloro-*p*-benzoquinone; Cl₄Q) supplied by Aldrich, were purified by vacuum sublimation. Benzonitrile (PhCN) was purchased from Wako Pure Chemical Industries, Ltd. and purified by successive distillation over P₂O₅.⁴⁰ Tetra-*n*-butylammonium perchlorate (TBAP), obtained from Fluka Fine Chemical, was recrystallized from ethanol and dried in vacuo prior to use. Tris(2,2'-bipyridine)iron(III) hexafluorophosphate, [Fe(bpy)₃](PF₆)₃, was prepared from a reaction between iron(II)sulfate heptahydrate and 2,2'-bipyridine followed by oxidation of the resulting iron(II) complex by ceric sulfate in aqueous H₂SO₄.⁴¹

Steady State Spectroscopic Apparatus. Steady state electronic absorption and fluorescence emission spectra of dilute solutions (10⁻⁴ to 10⁻⁶ M) of the samples were recorded using 1 cm path length rectangular quartz cells by means of an absorption spectrophotometer (Shimadzu UV–vis 2401PC) and F-4500 fluorescence spectrophotometer (Hitachi), respectively. Time-resolved fluorescence decays were measured by a Photon Technology International GL-3300 with a Photon Technology International GL-302 and a nitrogen laser/pumped dye laser system. The excitation wavelength of 530 nm was obtained by use of Coumarin 540A (Exciton Co, Ltd.) as a laser dye.

Phosphorescence Measurements. An N₂-saturated 2-methyl-tetrahydrofuran solution containing RU (5.2 × 10⁻⁶ M) at 77 K was excited at λ = 530 nm using a Cosmo System LVU-200S spectrometer. A photomultiplier (Hamamatsu Photonics model R5509-72) was used to detect emission in the near-infrared region (band path 2 mm).

Electrochemical Measurements. Measurements of cyclic voltammetry (CV) were made to determine the redox potentials of both RU and DQ using a ALS-630B electrochemical analyzer in a deaerated solvent containing 0.10 M tetra-*n*-butylammonium perchlorate (TBAP) as a supporting electrolyte at 298 K. A conventional three-electrode cell was used with a platinum working electrode and a platinum wire as a counter electrode.

Laser Flash Photolysis. For nanosecond laser flash photolysis experiments, deaerated PhCN solutions were excited by a Panther OPO pumped by Nd:YAG laser (Continuum, SLII-10, 4–6 ns fwhm) at λ = 530 nm. The photodynamics was monitored by continuous exposure to a xenon lamp (150 W) as

a probe light and a photomultiplier tube (Hamamatsu 2949) as a detector. The solution was deoxygenated by argon purging for 15 min prior to measurements.

Results and Discussion

ET Thermodynamics. The one-electron oxidation potential (*E*_{ox}) of rubrene (RU) and the one-electron reduction potentials (*E*_{red}) of *p*-benzoquinone derivatives were determined by the cyclic voltammograms measured in benzonitrile (PhCN). The *E*_{ox} value of RU was determined as 0.74 V (vs SCE) and the *E*_{red} values of *p*-benzoquinone derivatives were also determined as listed in Table 1. The value of the singlet excitation energy of RU (¹*E*^{*}) was determined from the average of absorption maximum (λ = 530 nm) and fluorescence maximum (λ = 560 nm) to be 2.28 eV. The value of the triplet excitation energy of RU (³*E*^{*}) was also determined from the phosphorescence maximum (λ = 990 nm) to be 1.25 eV (Figure S1).³⁶

The values of free energy change of photoinduced ET from ¹RU* to *p*-benzoquinone derivatives [Δ*G*_{et}(S); S denotes singlet] were determined from the *E*_{ox} value of RU and the *E*_{red} values of *p*-benzoquinone derivatives by eq 1.⁴² The electrostatic

$$\Delta G_{\text{et}}(\text{S}) = e(E_{\text{ox}} - E_{\text{red}}) - {}^1E^* \quad (1)$$

stabilization term is neglected in a highly polar solvent such as PhCN in eq 1. In the same way, the Δ*G*_{et}(S) values for other *p*-benzoquinone derivatives were determined as listed in Table 1.

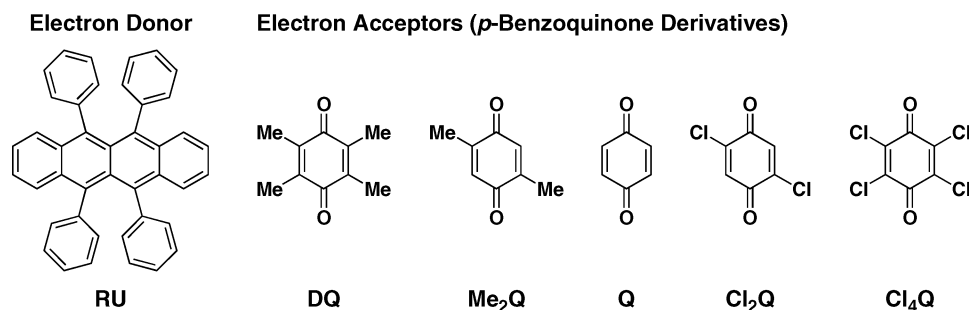
Steady State Spectroscopic Measurements. In PhCN solution, the UV–vis absorption spectra of the mixture of RU and DQ are observed to be the superposition of the corresponding spectra of the two reacting species. This indicates the lack of formation of any ground state of electron donor–acceptor complex under the present experimental conditions.

TABLE 1: One-Electron Reduction Potentials (*E*_{red}) of Electron Acceptors (*p*-Benzoquinone Derivatives), Free Energy Changes of Photoinduced ET [Δ*G*_{et}(S)] from ¹RU* to *p*-Benzoquinone Derivatives, and Rate Constants (*k*_{et}) of Photoinduced ET in PhCN at 298 K

no	electron acceptor ^d	<i>E</i> _{red} vs SCE in PhCN, V	Δ <i>G</i> _{et} (S), eV	<i>k</i> _{et} , ^b M ⁻¹ s ⁻¹
1	DQ	-0.97	-0.57	4.8 × 10 ⁹
2	Me ₂ Q	-0.79	-0.75	5.5 × 10 ⁹
3	Q	-0.61	-0.93	5.3 × 10 ⁹
4	Cl ₂ Q	-0.29	-1.25	6.0 × 10 ⁹
5	Cl ₄ Q	-0.09	-1.45	4.5 × 10 ⁹

^a Duroquinone (DQ), 2,5-dimethyl-*p*-benzoquinone (Me₂Q), *p*-benzoquinone (Q), 2,5-dichloro-*p*-benzoquinone (Cl₂Q), and *p*-chloranil (Cl₄Q). ^b Determined by the fluorescence lifetime measurements of RU in the presence of electron acceptors.

CHART 1



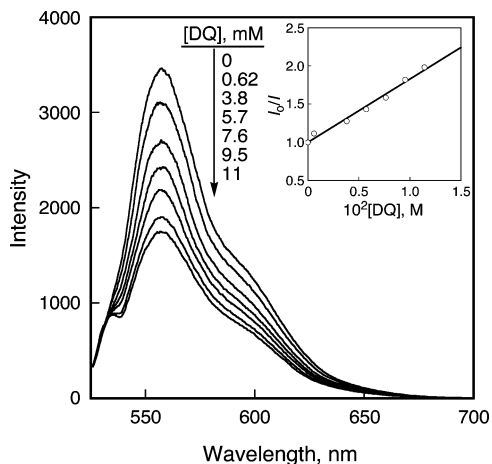


Figure 1. Fluorescence spectra of RU (2.9×10^{-5} M) in the presence of various concentrations of DQ (0 to 1.5×10^{-2} M) in deaerated PhCN ($\lambda_{\text{ex}} = 530$ nm). Inset: Plot of I_0/I at 560 nm vs $[\text{DQ}]$.

The steady state fluorescence emission of RU is quenched regularly throughout the entire band envelop with addition of the acceptor DQ in PhCN (Figure 1). It is relevant to point out here that as the fluorescence quenching of RU occurs in the region of DQ concentrations where the absorption spectrum of RU remains unaffected, the simple Stern–Volmer (SV) relation (eq 2) was employed³⁹ to analyze the fluorescence quenching

$$I_0/I = 1 + k_{\text{et}}\tau_0[\text{DQ}] \quad (2)$$

phenomena. Herein I_0 and I represent the fluorescence intensities of the donor RU in the absence and presence of the quencher DQ, the rate constant (k_{et}) is the bimolecular quenching rate constant, $[\text{DQ}]$ is the concentration of the quencher DQ, τ_0 is the fluorescence lifetime of RU in the absence of the quencher DQ, which was determined from the time-resolved fluorescence decay to be 15 ns in PhCN (Figure 2). The observed linearity in SV plot (inset of Figure 1) demonstrates in favor of the occurrence of dynamic quenching of fluorescence emission of RU in presence of DQ.

The fluorescence decay of RU was also measured in presence of DQ as shown in Figure 2a. The fluorescence lifetime (τ) was significantly shortened in the presence of DQ as compared with that in its absence. The bimolecular rate constant, k_{et} , obtained from the linear plot (Figure 2b) of τ_0/τ vs concentration of DQ ($4.8 \times 10^9 \text{ M}^{-1} \text{ s}^{-1}$) agrees within experimental error ($\pm 10\%$) with the value ($5.2 \times 10^9 \text{ M}^{-1} \text{ s}^{-1}$) determined from

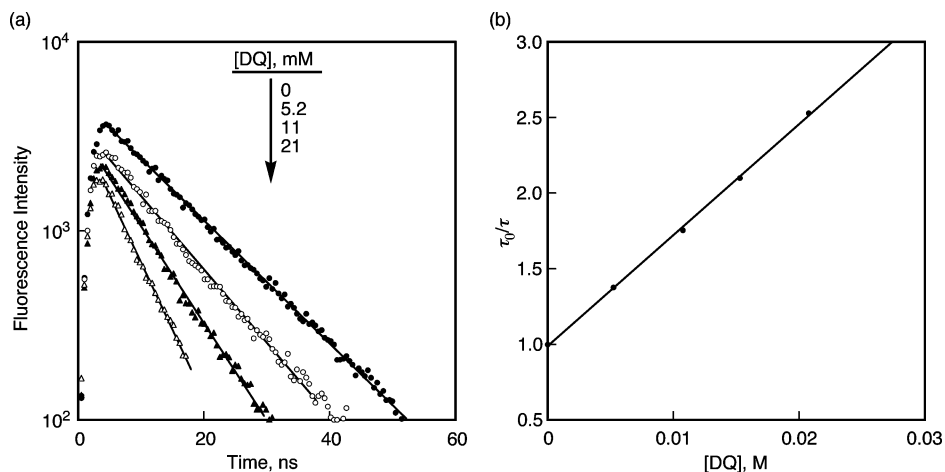


Figure 2. (a) Fluorescence decay time profiles of RU (1.6×10^{-5} M) at 560 nm with various concentration of DQ in deaerated PhCN at 298 K observed by excitation at 530 nm. (b) Plot of τ_0/τ vs $[\text{DQ}]$.

the steady state fluorescence intensity measurements in PhCN (inset of Figure 1). Similarly, the k_{et} values for other *p*-benzoquinone derivatives are determined from the plots of τ^{-1} vs concentrations of *p*-benzoquinone derivatives (see Supporting Information S2). The k_{et} values thus determined are listed in Table 1.

Transient Absorption Measurements. The direct evidence of the occurrence of photoinduced ET from ${}^1\text{RU}^*$ to *p*-benzoquinone derivatives is provided by the transient absorption spectral measurements with nanosecond laser flash photolysis. In the absence of *p*-benzoquinone (Q), the transient spectrum exhibits typical triplet–triplet absorption of RU (${}^3\text{RU}^*$) peaking at about 380, 420, 560, and 920 nm, together with bleaching at 530 nm due to RU (Figure 3a).⁴³ The decay of the absorbance at 420 nm due to ${}^3\text{RU}^*$ obeys first-order kinetics and the rate constant (k_{T}) the triplet decay to the ground state is determined as $2.7 \times 10^4 \text{ s}^{-1}$ at 298 K (Figure 3b).

Time-resolved nanosecond transient absorption spectra of RU with a series of electron acceptor, *p*-benzoquinone derivatives were measured by nanosecond laser flash photolysis in PhCN. At first glance, transient absorption spectra of RU in the presence of Q (Figure 4a) look similar to those in its absence (Figure 3a). However, the decay profiles are quite different. The absorbance at 420 nm due to ${}^3\text{RU}^*$ in absence of Q decays to nearly zero at 300 μs (Figure 3b), whereas the observed decay profile in the presence of Q (1.0×10^{-2} M) consists of two steps: the first fast decay and the second slower decay (Figure 4b,c). The first decay component obeys first-order kinetics and the rate constant is determined as $2.7 \times 10^4 \text{ s}^{-1}$ at 298 K (inset of Figure 4b).⁴⁴ This value agrees with the k_{T} value (Figure 3b). At 510 μs the transient absorption still remains as shown by open circles in Figure 4a. This spectrum agrees with that of $\text{RU}^{+\bullet}$ obtained by the one-electron oxidation of RU with $[\text{Fe}(\text{bpy})_3](\text{PF}_6)_3$ (Figure 5).⁴⁵ Thus, the transient absorption spectra of RU in the presence of Q and the time profile indicate that photoinduced ET from ${}^1\text{RU}^*$ to Q occurs to produce $\text{RU}^{+\bullet}$ and $\text{Q}^{\bullet-}$ in competition with the intersystem crossing (ISC) of ${}^1\text{RU}^*$ to ${}^3\text{RU}^*$. The absorption band due to $\text{Q}^{\bullet-}$ ($\lambda_{\text{max}} = 420 \text{ nm}$)⁴⁶ is overlapped with that of $\text{RU}^{+\bullet}$.

The second slower decay curve in Figure 4c obeys second-order kinetics and it can be analyzed by the second-order plot (inset of Figure 4c). The rate constant (k_{bet}) of intermolecular BET from $\text{Q}^{\bullet-}$ to $\text{RU}^{+\bullet}$ is determined from a slope of the inset of Figure 4c as $5.2 \times 10^9 \text{ M}^{-1} \text{ s}^{-1}$ in PhCN at 298 K. This value agrees with a diffusion rate constant (k_{diff}) in PhCN ($5.6 \times 10^9 \text{ M}^{-1} \text{ s}^{-1}$).⁴⁷ No rise in the triplet absorption is observed

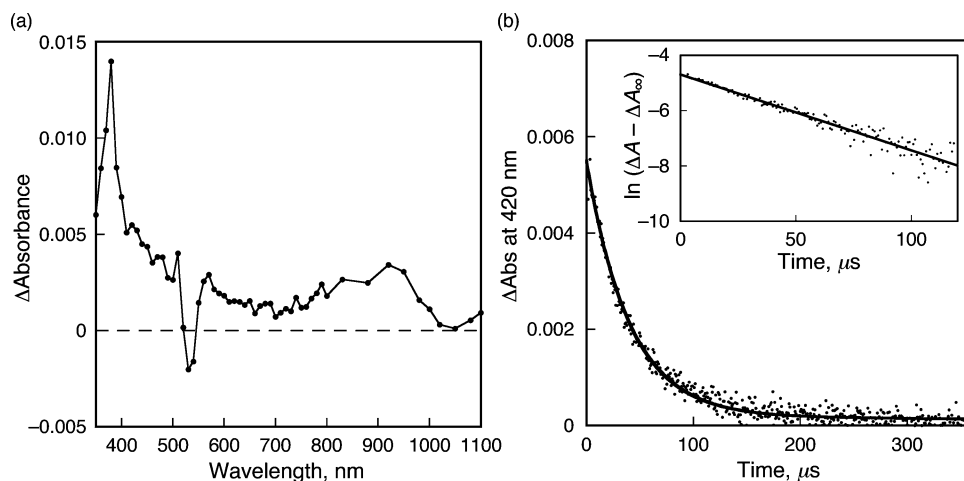


Figure 3. (a) Transient absorption spectra of RU (6.0×10^{-5} M) in deaerated PhCN at 298 K taken at $3.2 \mu\text{s}$ (●) after nanosecond laser excitation at 530 nm. (b) Time profile at 420 nm. Inset: first-order plot.

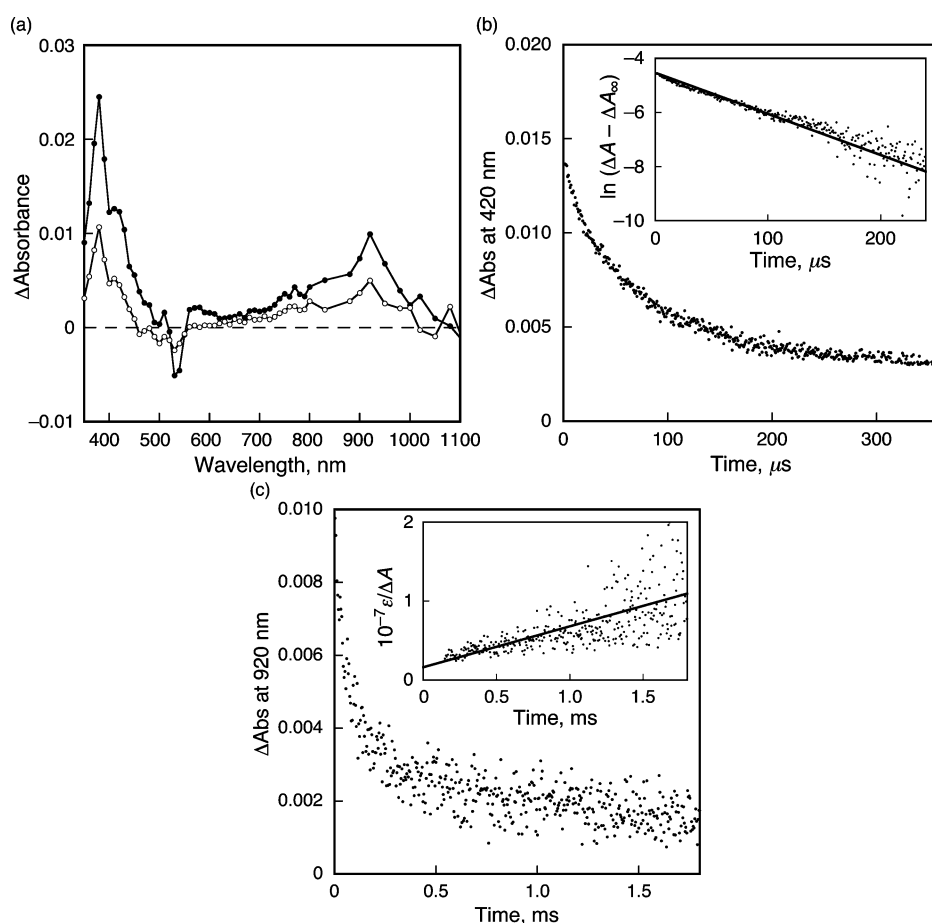


Figure 4. (a) Transient absorption spectra of RU (6.5×10^{-5} M) in the presence of Q (1.0×10^{-2} M) in deaerated PhCN at 298 K taken at $16 \mu\text{s}$ (●) and $510 \mu\text{s}$ (○) after nanosecond laser excitation at 530 nm. (b) Decay time profile at 420 nm of RU (6.5×10^{-5} M) in the presence of Q (1.0×10^{-2} M) in the 0–360 μs range. Inset: first-order plots for the fast component ($\Delta A_{\infty} = 0.0031$). (c) Decay time profile at 920 nm of RU (6.5×10^{-5} M) in the presence of Q (1.0×10^{-2} M) in the 0–1.8 ms range. Inset: second-order plot for the slow component.

during the intermolecular BET process. This clearly indicates that the intermolecular BET results in formation of the ground state reactant RU rather than the triplet excited state ${}^3\text{RU}^*$, although the triplet energy of ${}^3\text{RU}^*$ (1.25 eV) is lower than the driving force of intermolecular BET from $\text{Q}^{\bullet-}$ to $\text{RU}^{\bullet+}$ to produce the ground state of RU (1.35 eV). Similar results were obtained for photoinduced ET of RU with DQ and Me_2Q (see Supporting Information S3 and S4, respectively). In each case, the photoexcitation results in formation of $\text{RU}^{\bullet+}$ and $\text{DQ}^{\bullet-}$ (or $\text{Me}_2\text{Q}^{\bullet-}$) as well as ${}^3\text{RU}^*$. The decay of ${}^3\text{RU}^*$ is followed by

the slower intermolecular BET, which results in formation of the ground state of RU rather than ${}^3\text{RU}^*$.

The energy diagram of photoinduced ET from ${}^1\text{RU}^*$ to electron acceptors ($A = \text{DQ}, \text{Me}_2\text{Q}$ and Q) and the BET process is summarized in Scheme 1a. Photoinduced ET from ${}^1\text{RU}^*$ to A results in formation of $\text{RU}^{\bullet+}$ and $A^{\bullet-}$ in competition of ISC to ${}^3\text{RU}^*$. Although the triplet energy of ${}^3\text{RU}^*$ is lower than the CS state of $\text{RU}^{\bullet+}$ and $A^{\bullet-}$, the BET results in formation of the ground state of RU rather than ${}^3\text{RU}^*$. The reason for this is discussed later.

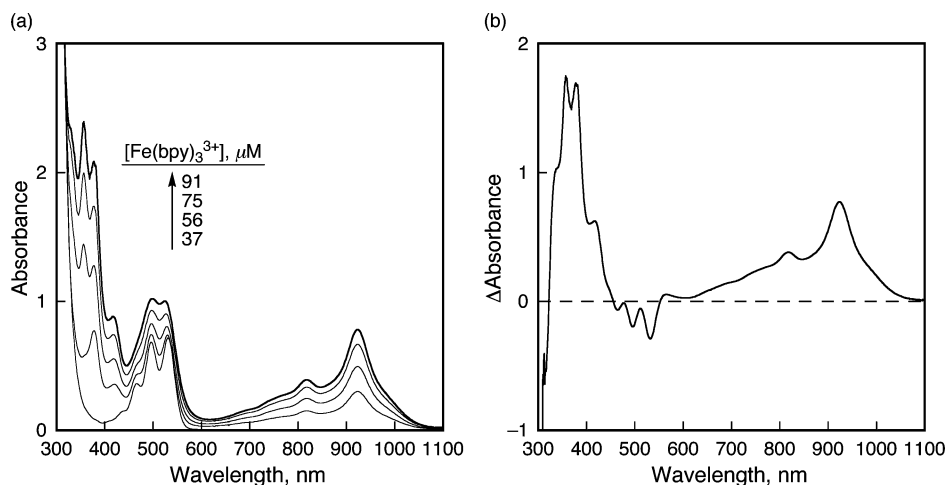
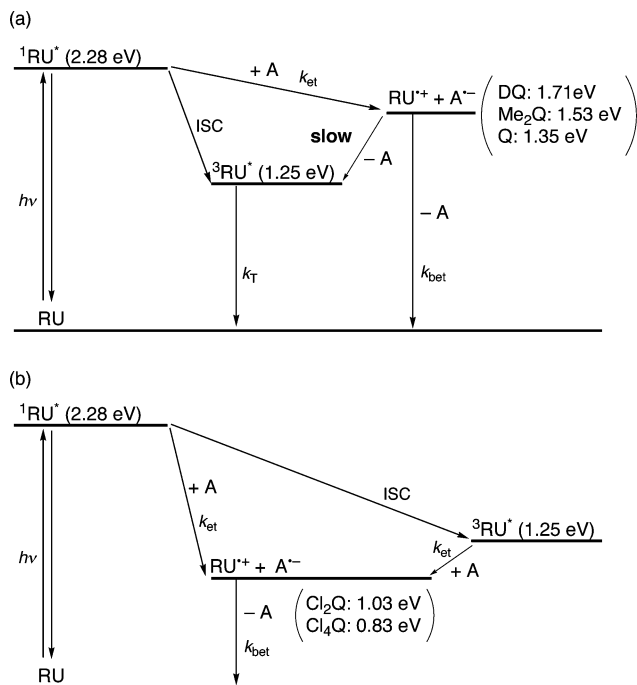


Figure 5. (a) UV-vis spectral change upon addition of $[\text{Fe}(\text{bpy})_3](\text{PF}_6)_3$ ($\text{bpy} = 2,2'$ -bipyridine) in deaerated MeCN to a PhCN solution containing RU (9.1×10^{-5} M) at 298 K. (b) Difference absorption spectrum of RU^{*+} obtained upon UV-vis spectral change after addition of $[\text{Fe}(\text{bpy})_3](\text{PF}_6)_3$ (9.1×10^{-5} M) to RU (9.1×10^{-5} M) solution in PhCN at 298 K.

SCHEME 1: (a) Energy Diagram of Photoinduced ET from Excited State of RU to *p*-Benzoquinone Derivatives [(a) DQ, Me₂Q, Q; (b) Cl₂Q, Cl₄Q]



When *p*-benzoquinone derivatives with electron-withdrawing substituents such as Cl_4Q are employed as electron acceptors, photoinduced ET not only from $^1\text{RU}^*$ but also from $^3\text{RU}^*$ to Cl_4Q becomes thermodynamically feasible, because the triplet energy of $^3\text{RU}^*$ (1.25 eV) is larger than the driving force of intermolecular BET from $\text{Cl}_4\text{Q}^{\bullet-}$ to RU^{*+} to produce the ground state of RU (0.83 eV) as shown in Scheme 1b. In such a case, $^3\text{RU}^*$ is converted to RU^{*+} by electron transfer from $^3\text{RU}^*$ to Cl_4Q , when transient absorption spectra due to RU^{*+} and $\text{Cl}_4\text{Q}^{\bullet-}$ are observed at 16 μs after nanosecond laser excitation as shown in Figure 6a. The absorption band due to $\text{Cl}_4\text{Q}^{\bullet-}$ ($\lambda_{\text{max}} = 450$ nm)⁴⁸ is overlapped with that due to RU^{*+} . The decay time profile of absorbance at 920 nm due to RU^{*+} obeys second-order kinetics without exhibiting the initial first-order decay due to $^3\text{RU}^*$ (Figure 6b). The k_{bet} value is determined from the second-order plot (inset of Figure 6b) as 5.4×10^9 $\text{M}^{-1} \text{s}^{-1}$.

The triplet pathway of photoinduced ET from $^3\text{RU}^*$ to Cl_4Q becomes dominant when low concentrations of Cl_4Q are employed. Figure 7 shows the rise in absorbance at 450 nm due to $\text{Cl}_4\text{Q}^{\bullet-}$, where absorbance due to RU^{*+} is overlapped, after laser excitation of a PhCN solution of RU (7.0×10^{-5} M) and Cl_4Q [(0.6–3.0) $\times 10^{-4}$ M]. Under such experimental conditions, the decay of absorbance due to $\text{Cl}_4\text{Q}^{\bullet-}$ and RU^{*+} is negligible. The rate of rise in absorbance obeys pseudo-first-order kinetics and the observed pseudo-first-order rate constant (k_{obs}) increases linearly with increasing concentration of Cl_4Q (inset of Figure 7). The k_{et} value of photoinduced ET from $^3\text{RU}^*$ to Cl_4Q is determined from the slope of the linear plot of k_{obs} vs concentration of Cl_4Q as $(6.7 \pm 0.7) \times 10^9$ $\text{M}^{-1} \text{s}^{-1}$. Similarly the k_{et} value of photoinduced ET from $^3\text{RU}^*$ to Cl_2Q was determined as $(1.8 \pm 0.2) \times 10^9$ $\text{M}^{-1} \text{s}^{-1}$ (see Supporting Information S6).

The free energy changes of photoinduced ET from $^3\text{RU}^*$ to *p*-benzoquinone derivatives ($\Delta G_{\text{et}}(\text{T})$; T denotes triplet) and BET (ΔG_{bet}) are determined by eqs 3 and 4, respectively.⁴⁹ The triplet

$$\Delta G_{\text{et}}(\text{T}) = e[E_{\text{ox}}(\text{D}/\text{D}^{*+}) - E_{\text{red}}(\text{A}^{\bullet-}/\text{A})] - ^3E^* \quad (3)$$

$$\Delta G_{\text{bet}} = -e[E_{\text{ox}}(\text{D}/\text{D}^{*+}) - E_{\text{red}}(\text{A}^{\bullet-}/\text{A})] \quad (4)$$

excited energy ($^3E^*$) of RU is taken as 1.25 eV (vide supra). The $\Delta G_{\text{et}}(\text{T})$ and ΔG_{bet} values are listed in Table 2 together with the k_{et} and k_{bet} values.

Photoinduced ET from $^1\text{RU}^*$ (or $^3\text{RU}^*$) to an electron acceptor (A) may occur as shown in Scheme 2, where k_{12} and k_{21} are the diffusion rate constant and the dissociation rate constant in the encounter complex ($\text{RU}^* \text{A}$), k_{ET} and k_{bet} are the first-order rate constant of the forward ET from RU^* to A in the encounter complex and the second-order rate constant of BET to the ground state, respectively.⁵⁰ The observed second-order rate constant of forward ET (k_{et}) is given by eq 5. The

$$k_{\text{et}} = k_{\text{ET}}k_{12}/(k_{21} + k_{\text{ET}}) \quad (5)$$

dependence of k_{ET} on the ET driving force [$-\Delta G_{\text{et}}$] for adiabatic outer-sphere ET has well been established by Marcus as given by eq 6, where k_{B} is the Boltzmann constant, h is the Planck

$$k_{\text{ET}} = (k_{\text{B}}T/h)\exp[-(\lambda/4)(1 + \Delta G_{\text{et}}/\lambda)^2/k_{\text{B}}T] \quad (6)$$

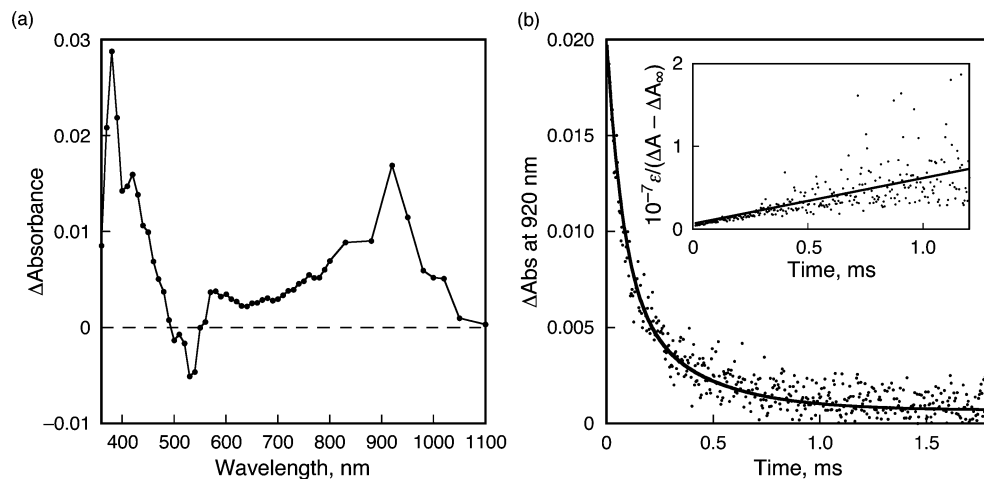


Figure 6. (a) Transient absorption spectra of RU (6.8×10^{-5} M) in the presence of Cl₄Q (5.0×10^{-3} M) in deaerated PhCN at 298 K taken at 16 μ s after nanosecond laser excitation at 530 nm. (b) Decay time profile at 920 nm of RU (6.8×10^{-5} M) in the presence of Cl₄Q (5.0×10^{-3} M). Inset: second-order plot.

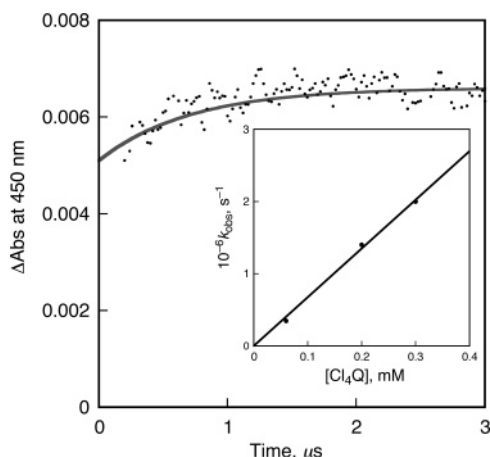


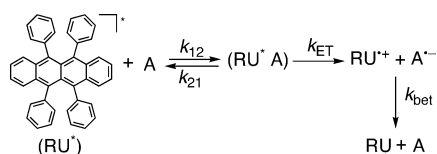
Figure 7. Decay time profile of absorbance at 450 nm after laser excitation at 530 nm of a PhCN solution of RU (7.0×10^{-5} M) with Cl₄Q (2.0×10^{-4} M) at 298 K. Inset: Plot of k_{obs} vs [Cl₄Q].

TABLE 2: Free Energy Changes of Photoinduced ET from ³RU* to *p*-Benzoquinone Derivatives [$\Delta G_{\text{et}}(\text{T})$] and Back Electron Transfer (BET) to the Ground State (ΔG_{bet}) and the Rate Constants of Photoinduced ET (k_{et}) and BET (k_{bet}) in PhCN

no	electron acceptor	$\Delta G_{\text{et}}(\text{T}),^a$ eV	$\Delta G_{\text{bet}},^b$ eV	$k_{\text{et}},^c$ $\text{M}^{-1} \text{s}^{-1}$	$k_{\text{bet}},^c$ $\text{M}^{-1} \text{s}^{-1}$
1	DQ	0.46	-1.71		4.1×10^9
2	Me ₂ Q	0.28	-1.53		5.0×10^9
3	Q	0.10	-1.35		5.2×10^9
4	Cl ₂ Q	-0.22	-1.03	1.8×10^9	5.4×10^9
5	Cl ₄ Q	-0.42	-0.83	6.7×10^9	5.4×10^9

^a Determined from eq 3. ^b Determined from eq 4. ^c Determined using the molar absorption coefficients of RU⁺ at 920 nm ($\epsilon = 8500 \text{ M}^{-1} \text{ cm}^{-1}$). The experimental error is within $\pm 5\%$.

SCHEME 2



constant, and λ is the reorganization energy of ET.^{20,34} From eqs 5 and 6 is derived eq 7, where $Z = [(kT/h)(k_{12}/k_{21})]$ is the collision frequency that is taken as $1 \times 10^{11} \text{ M}^{-1} \text{ s}^{-1}$.⁴⁹ The k_{12} values in PhCN is taken $5.6 \times 10^9 \text{ M}^{-1} \text{ s}^{-1}$.⁴⁷

$$k_{\text{et}} = k_{12} Z \exp[-(\lambda/4)(1 + \Delta G_{\text{et}}/\lambda)^2/k_{\text{B}}T] / (k_{12} + Z \exp[-(\lambda/4)(1 + \Delta G_{\text{et}}/\lambda)^2/k_{\text{B}}T]) \quad (7)$$

The driving force dependence of the k_{et} values of photoinduced ET from both ³RU* (open squares) and ¹RU* to *p*-benzoquinone derivatives (open circles and closed triangles) is shown in Figure 8 including the driving force dependence of the k_{bet} values. At least two different λ values are required to fit all the rate constants, i.e., the k_{et} values of photoinduced ET from both ³RU* and ¹RU* to *p*-benzoquinone derivatives and the k_{bet} values using eq 7. The k_{et} values of photoinduced ET from ³RU* to Cl₂Q and Cl₄Q including the k_{et} values of photoinduced ET from ¹RU* to DQ, Me₂Q and Q (open circles in Figure 8) are best fitted by the solid line in Figure 8 with the λ value of 0.81 eV. However, significant deviation from the calculated solid line with $\lambda = 0.81$ eV is observed for the k_{et} values of photoinduced ET from ¹RU* to Cl₂Q and Cl₄Q (closed triangles) with a driving force larger than 1.0 eV as well as the k_{bet} values which have also a driving force larger than 1.0 eV. These values are much larger than the calculated solid line with $\lambda = 0.81$ eV. However, they can be best fitted with $\lambda = 1.22$ eV, as shown by the broken line in Figure 8.⁵¹

With regard to BET to generate ³RU*, the calculated rate constants for BET from DQ⁻, Me₂Q⁻, and Q⁻ to RU⁺ with $\lambda = 1.22$ eV are shown by the arrows (a, b, and c, respectively) on the broken line in Figure 8. These values are much smaller than the observed k_{bet} values. This is consistent with the experimental results in Figure 4, where the BET process affords the ground state of RU rather than the triplet excited state (³RU*).⁵²

The solvent reorganization energy λ_s is known to vary depending on the distance between an electron donor and an acceptor as given by eq 8, where r_1 and r_2 are the radii of the

$$\lambda_s = e^2(1/2r_1 + 1/2r_2 - 1/r_{12})(1/n^2 - 1/\epsilon) \quad (8)$$

reactants, r_{12} is the reaction distance, ϵ is the dielectric constant, and n is the refractive index.^{34,53} The RU and DQ radii were reported as crystal structures, and according to those results, the radii were 13 Å⁵⁴ and 6.8 Å,⁵⁵ respectively. If the reaction distance is assumed as infinite, the term $-1/2r_{12}$ in eq 8 is negligible. In such a case, the maximum λ_s value is estimated as 1.25 eV, which is comparable with the λ value (1.22 eV) for photoinduced ET and BET at a driving force larger than 1.0

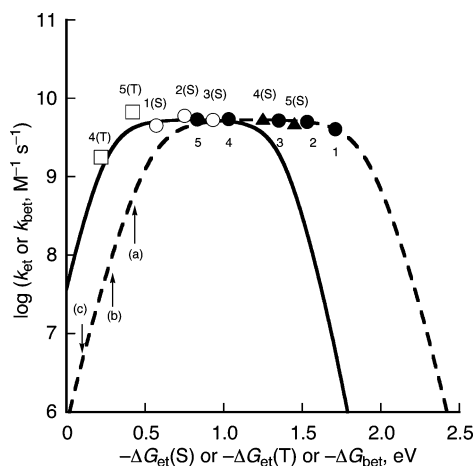


Figure 8. Driving force ($-\Delta G_{\text{et}}(\text{S})$ or $-\Delta G_{\text{et}}(\text{T})$ or $-\Delta G_{\text{bet}}$) dependence of $\log k_{\text{et}}$ for intermolecular photoinduced ET from $^1\text{RU}^*$ to *p*-benzoquinone derivatives [(○) for DQ, Me_2Q and Q; (▲) for Cl_2Q and Cl_4Q] and from $^3\text{RU}^*$ to Cl_2Q and Cl_4Q (□) (solid line) and $\log k_{\text{bet}}$ for BET (●) (broken line) in PhCN at 298 K. The solid and broken lines are drawn on the basis of eq 7 with $\lambda = 0.81$ and 1.22 eV, respectively. Numbers refer to the electron acceptors in Tables 1 and 2. The arrow represents the predicted rate constant for the intermolecular BET from (a) $\text{DQ}^{\bullet-}$, (b) $\text{Me}_2\text{Q}^{\bullet-}$, and (c) $\text{Q}^{\bullet-}$ to $\text{RU}^{+\bullet}$ to produce $^3\text{RU}^*$ from eq 6 with $\lambda = 1.22$ eV.

eV. This suggests that the λ_{s} value increases with increasing the ET driving force as the r_{12} value increases, when it becomes more difficult to reach the Marcus inverted region ($-\Delta G_{\text{et}}$ or $-\Delta G_{\text{bet}} > \lambda$). Thus, an increase in the r_{12} value with increasing the ET or BET driving force is the main reason why the k_{et} or k_{bet} value remains to be diffusion-limited even at a large driving force of ET or BET without falling into the Marcus inverted region. It should be noted, however, such an increase in the r_{12} value with increasing the ET driving force is limited by an increase in non-adiabaticity of ET at a longer distance.

In conclusion, photoinduced ET from $^1\text{RU}^*$ to *p*-benzoquinone derivatives and BET occurs at a longer distance between an electron donor and acceptor as the driving force increases, accompanied by an increase in the solvent reorganization energy. Such an increase in the solvent reorganization energy with increasing the ET or BET driving force has precluded the slowdown of the intermolecular ET rate, which would otherwise occur in the Marcus inverted region at a large ET driving force. Thus, the Marcus inverted region is observed only when electron donors and acceptors with extremely small λ values such as fullerenes are employed for intermolecular ET reactions.³¹ In contrast with intermolecular ET, the Marcus inverted region is commonly observed in intramolecular ET of electron donor-acceptor linked molecules with a fixed distance. When intramolecular BET to the ground state has a much larger driving force than the corresponding BET to the triplet excited state, the triplet excited state is often formed because the former rate is slowed down in the Marcus inverted region as compared with the latter rate in the Marcus normal region.^{27,56,57} However, this is not the case in intermolecular BET from the radical anions of *p*-benzoquinone derivatives to $\text{RU}^{+\bullet}$, which afford the ground state of RU rather than $^3\text{RU}^*$ even when the intermolecular BET to $^3\text{RU}^*$ is thermodynamically feasible. Such a preference to the intermolecular BET to the ground state of RU with a larger driving force than the BET to the triplet excited state $^3\text{RU}^*$ results from an increase in the solvent reorganization energy with an increase in the BET driving force.

Acknowledgment. This work was supported by a Grant-in-Aid (Nos. 19205019 and 19750034) from the Ministry of Education, Culture, Sports, Science and Technology, Japan. M.M. expresses his special thanks for The Global COE (center of excellence) program "Global Education and Research Center for Bio-Environmental Chemistry" of Osaka University. T.G. gratefully acknowledges the Japan Society for the Promotion of Science (JSPS) for inviting him in FY2006 JSPS Invitation Fellowship Program for Research in Japan (short term).

Supporting Information Available: Phosphorescence spectrum, τ^{-1} vs concentration plots, absorption spectra, and plot of k_{obs} vs $[\text{Cl}_2\text{Q}]$. This material is available free of charge via the Internet at <http://pubs.acs.org>.

References and Notes

- (1) (a) Gould, I. R.; Young, R. H.; Farid, S. In *Photochemical Processes in Organized Molecular Systems*; Honda, K., Ed.; North Holland: Amsterdam, 1991; p 19. (b) Mataga, N. In *Dynamics and Mechanisms of Photoinduced Electron Transfer and Related Phenomena*; Mataga, N., Okada, T., Masuhara, H., Eds.; North-Holland: Amsterdam, 1992; p 3.
- (2) Ebersson, L. *Electron-Transfer Reactions in Organic Chemistry*; Springer-Verlag: New York, 1987.
- (3) Rathore, R.; Kochi, J. K. *Adv. Phys. Org. Chem.* **2000**, *35*, 193.
- (4) Pal, S. K.; Bhattacharya, T.; Misra, T.; Saini, R. D.; Ganguly, T. *J. Phys. Chem. A* **2003**, *107*, 10243.
- (5) Julliard, M.; Chanon, M. *Chem. Rev.* **1983**, *83*, 425–506.
- (6) Rosokha, S. V.; Lü, J.-M.; Newton, M. D.; Kochi, J. K. *J. Am. Chem. Soc.* **2005**, *127*, 7411.
- (7) (a) D'Souza, F.; Ito, O. *Coord. Chem. Rev.* **2005**, *249*, 1410. (b) D'Souza, F.; Chitta, R.; Gadde, S.; Rogers, L. M.; Karr, P. A.; Zandler, M. E.; Sandanayaka, A. S. D.; Araki, Y.; Ito, O. *Chem.-Eur. J.* **2007**, *13*, 916.
- (8) (a) Müller, F.; Mattay, J. *Chem. Rev.* **1993**, *93*, 99–117. (b) Mattay, J. *Angew. Chem., Int. Ed. Engl.* **1987**, *26*, 825.
- (9) Kavarnos, G. J.; Turro, N. J. *Chem. Rev.* **1986**, *86*, 401.
- (10) Balzani, V.; Moggi, L.; Manfrin, M. F.; Bolletta, F. *Coord. Chem. Rev.* **1975**, *15*, 321.
- (11) Lewis, F. D.; Letsinger, R.; Wasielewski, M. R. *Acc. Chem. Res.* **2001**, *34*, 159.
- (12) Fukuzumi, S.; Itoh, S. In *Advances in Photochemistry*; Neckers, D. C., Volman, D. H., von Bünau, G., Eds.; Wiley: New York, 1998; Vol. 25, pp 107–172.
- (13) (a) Fukuzumi, S. *Org. Biomol. Chem.* **2003**, *1*, 609. (b) Fukuzumi, S. *Bull. Chem. Soc. Jpn.* **1997**, *70*, 1.
- (14) Pal, S. K.; Sahu, T.; Misra, T.; Mallick, P. K.; Paddon-Row, M. N.; Ganguly, T. *J. Phys. Chem. A* **2004**, *108*, 10395.
- (15) Van der Boom, T.; Hayes, R. T.; Zhao, Y.; Bushard, P. J.; Weiss, E. A.; Wasielewski, M. R. *J. Am. Chem. Soc.* **2002**, *124*, 9582.
- (16) Bell, T. D. M.; Ghiggino, K. P.; Jolliffe, K. A.; Ranasinghe, M. G.; Langford, S. J.; Shephard, M. J.; Paddon-Row, M. N. *J. Phys. Chem. A* **2002**, *106*, 10079.
- (17) Heinen, U.; Berthold, T.; Kothe, G.; Stavitski, E.; Galili, T.; Levanon, H.; Wiederrecht, G.; Wasielewski, M. R. *J. Phys. Chem. A* **2002**, *106*, 1933.
- (18) (a) Bock, C. R.; Meyer, T. J.; Whitten, D. G. *J. Am. Chem. Soc.* **1975**, *97*, 2909. (b) Ballardini, R.; Varani, G.; Indelli, M. T.; Scandola, F.; Balzani, V. *J. Am. Chem. Soc.* **1978**, *100*, 7219.
- (19) (a) Fukuzumi, S.; Hironaka, K.; Nishizawa, N.; Tanaka, T. *Bull. Chem. Soc. Jpn.* **1983**, *56*, 2220. (b) Fukuzumi, S.; Kuroda, S.; Tanaka, T. *J. Am. Chem. Soc.* **1985**, *107*, 3020. (c) Fukuzumi, S.; Koumitsu, S.; Hironaka, K.; Tanaka, T. *J. Am. Chem. Soc.* **1987**, *109*, 305. (d) Fukuzumi, S.; Ohkubo, K.; Suenobu, T.; Kato, K.; Fujitsuka, M.; Ito, O. *J. Am. Chem. Soc.* **2001**, *123*, 8459.
- (20) (a) Marcus, R. A. *Annu. Rev. Phys. Chem.* **1964**, *15*, 155. (b) Marcus, R. A.; Sutin, N. *Biochim. Biophys. Acta* **1985**, *811*, 265. (c) Marcus, R. A. *Angew. Chem., Int. Ed. Engl.* **1993**, *32*, 1111.
- (21) (a) Miller, J. R.; Calcaterra, L. T.; Closs, G. L. *J. Am. Chem. Soc.* **1984**, *106*, 3047. (b) Closs, G. L.; Miller, J. R. *Science* **1988**, *240*, 440.
- (22) Gould, I. R.; Farid, S. *Acc. Chem. Res.* **1996**, *29*, 522.
- (23) (a) McLendon, G. *Acc. Chem. Res.* **1988**, *21*, 160. (b) Winkler, J. R.; Gray, H. B. *Chem. Rev.* **1992**, *92*, 369. (c) McLendon, G.; Hake, R. *Chem. Rev.* **1992**, *92*, 481.
- (24) Mataga, N.; Miyasaka, H. In *Electron Transfer from Isolated Molecules to Biomolecules Part 2*; Jortner, J., Bixon, M., Eds.; Wiley: New York, 1999; p 431.
- (25) (a) Wasielewski, M. R. In *Photoinduced Electron Transfer*; Fox, M. A., Chanon, M., Eds.; Elsevier: Amsterdam, 1988; Part A, p 161. (b)

- Wasielowski, M. R. *Chem. Rev.* **1992**, *92*, 435. (c) Jordan, K. D.; Paddon-Row, M. N. *Chem. Rev.* **1992**, *92*, 395.
- (26) (a) Gust, D.; Moore, T. A. In *The Porphyrin Handbook*; Kadish, K. M., Smith, K. M., Guillard, R., Eds.; Academic Press: San Diego, CA, 2000; Vol. 8, pp 153–190. (b) Gust, D.; Moore, T. A.; Moore, A. L. *Acc. Chem. Res.* **2001**, *34*, 40. (c) Paddon-Row, M. N. *Acc. Chem. Res.* **1994**, *27*, 18.
- (27) Fukuzumi, S.; Guldi, D. M. In *Electron Transfer in Chemistry*; Balzani, V. Ed.; Wiley-VCH: Weinheim, 2001; Vol. 2, pp 270–337.
- (28) Wasielowski, M. R.; Niemczyk, M. P.; Svec, W. A.; Pewitt, E. P. *J. Am. Chem. Soc.* **1985**, *107*, 5562.
- (29) Harrison, R. J.; Pearce, B.; Beddard, G. S.; Cowan, J. A.; Sanders, J. K. M. *Chem. Phys.* **1987**, *116*, 429.
- (30) Smitha, M. A.; Prasad, E.; Gopidas, K. R. *J. Am. Chem. Soc.* **2001**, *123*, 1159.
- (31) Fukuzumi, S.; Ohkubo, K.; Imahori, H.; Guldi, D. M. *Chem. Eur. J.* **2003**, *9*, 1585.
- (32) Vauthey, E. *J. Photochem. Photobiol. A: Chem.* **2006**, *179*, 1.
- (33) Efrima, S.; Bixon, M. *Chem. Phys. Lett.* **1974**, *25*, 34.
- (34) Brunschwig, B. S.; Ehrenson, S.; Sutin, N. *J. Am. Chem. Soc.* **1984**, *106*, 6858.
- (35) (a) Tachiya, M.; Murata, S. *J. Phys. Chem.* **1992**, *96*, 8441. (b) Barzykin, A. V.; Frantsuzov, P. A.; Seki, K.; Tachiya, M. *Adv. Chem. Phys.* **2002**, *123*, 511.
- (36) The same ${}^3E^*$ value was reported previously, see: (a) Visco, R. E.; Chandross, E. A. *Electrochim. Acta* **1968**, *13*, 1187. (b) Chang, J.; Hercules, D. M.; Roe, D. K. *Electrochim. Acta* **1968**, *13*, 1197. (c) Faulkner, L. R.; Tachikawa, H.; Bard, A. J. *J. Am. Chem. Soc.* **1972**, *94*, 691. (d) Yeh, L.-S. R.; Bard, A. J. *Chem. Phys. Lett.* **1976**, *44*, 339.
- (37) Ushida, K.; Yoshida, Y.; Kozawa, T.; Tagawa, S.; Kira, A. *J. Phys. Chem. A* **1999**, *103*, 4680.
- (38) (a) Weidemaier, K.; Tavernier, H. L.; Swallen, S. F.; Fayer, M. D. *J. Phys. Chem. A* **1997**, *101*, 1887. (b) Swallen, S. F.; Weidemaier, K.; Tavernier, H. L.; Fayer, M. D. *J. Phys. Chem.* **1996**, *100*, 8106.
- (39) Tsai, Y.; Jou, J. *Appl. Phys. Lett.* **2006**, *89*, 243521.
- (40) Armarego, W. L. F.; Perrin, D. D. *Purification of Laboratory Chemicals*, 4th ed.; Butterworth-Heinemann: Boston, 1996.
- (41) (a) Wong, C. L.; Kochi, J. K. *J. Am. Chem. Soc.* **1979**, *101*, 5593. (b) Fukuzumi, S.; Wong, C. L.; Kochi, J. K. *J. Am. Chem. Soc.* **1980**, *102*, 2928.
- (42) (a) Rehm, A.; Weller, A. *Ber. Bunsenges Phys. Chem.* **1969**, *73*, 834. (b) Rehm, A.; Weller, A. *Isr. J. Chem.* **1970**, *8*, 259.
- (43) Yildiz, A.; Kissinger, P. T.; Reilley, C. N. *J. Chem. Phys.* **1968**, *49*, 1403.
- (44) Forward ET process from ${}^1\text{RU}^*$ to Q could not be observed by nanosecond laser flash photolysis because the ET rate is faster than the time scale of detection limit.
- (45) Absorption spectrum of RU^{+} has been reported. Shida, T. *Electronic Absorption Spectra of Radical Ions*; Elsevier; New York, 1988.
- (46) Fukuzumi, S.; Nakanishi, I.; Maruta, J.; Yorisue, T.; Suenobu, T.; Itoh, S.; Arakawa, R.; Kadish, R. M. *J. Am. Chem. Soc.* **1998**, *120*, 6673.
- (47) Fukuzumi, S.; Suenobu, T.; Patz, M.; Hirasaka, T.; Itoh, S.; Fujitsuka, M.; Ito, O. *J. Am. Chem. Soc.* **1998**, *120*, 8060.
- (48) Fukuzumi, S.; Nishizawa, N.; Tanaka, T. *J. Org. Chem.* **1984**, *49*, 3571.
- (49) The distance dependence of ET energies in polar solvent such as PhCN may be negligible.⁴²
- (50) Kavarnos, G. J. *Fundamentals of Photoinduced Electron Transfer*; Wiley-VCH: New York, 1993.
- (51) The λ value may increase gradually with an increase in the reaction distance (Δr_{12}). We have chosen the two extreme cases (the smallest and the largest ones) in Figure 8. However, the exact dependence of λ on r_{12} has yet to be clarified. The λ value for BET process depends on the reaction distance.
- (52) Spin conversion of the $\text{RU}^{+}/\text{Q}^{\bullet-}$ ion pair is generally faster than the intermolecular BET processes. Thus, the spin conversion process should not be rate determining step; see: (a) Piotrowiak, P. In *Photochemistry and Radiation Chemistry: Complementary Methods for the Study of Electron Transfer*; Wishart, J. F., Nocera, D. G., Ed.; Advances in Chemistry Series, No. 254; American Chemical Society: Washington, DC, 1998; pp 219–230. (b) Kuciauskas, D.; Liddell, P.; Moore, A.; Moore, T.; Gust, D. *J. Am. Chem. Soc.* **1998**, *120*, 10880. (c) Grzeskowiak, K. N.; Smirnov, S. N.; Braun, C. L. *J. Phys. Chem.* **1994**, *98*, 5661. (d) Vlasiouk, I.; Smirnov, S.; Kutzki, O.; Wedel, M.; Montforts, F.-P. *J. Phys. Chem. B* **2002**, *106*, 8657.
- (53) (a) Shen, X.; Lind, J.; Merenyi, G. *J. Phys. Chem.* **1987**, *91*, 4403. (b) Merenyi, G.; Lind, J.; Shen, X. *J. Phys. Chem.* **1988**, *92*, 134. (c) Shen, X.; Lind, J.; Eriksen, T. E.; Merenyi, G. *J. Chem. Soc., Perkin Trans. 2* **1989**, 555.
- (54) (a) Munakata, M.; Wu, L. P.; Kuroda-Sowa, T.; Maekawa, M.; Suenaga, Y.; Ning, G. L.; Kojima, T. *J. Am. Chem. Soc.* **1998**, *120*, 8610. (b) Wheeler, L. O.; Bard, A. J. *J. Phys. Chem.* **1967**, *71*, 4513. (c) Avoyan, R. L.; Kitaigorodskii, I.; Struchkov, Y. T. *J. Struct. Chem.* **1964**, *5*, 390.
- (55) (a) Lu, J.-M.; Rosokha, S. V.; Neretin, I. S.; Kochi, J. K. *J. Am. Chem. Soc.* **2006**, *128*, 16708. (b) van Bolhuis, F.; Kiers, C. T. *Acta Crystallogr., Sect. B* **1978**, *34*, 1015. (c) Rabinovich, D.; Schmidt, G. M.; Ubel, E. *J. Chem. Soc. B* **1967**, 131. (d) Aleksandrov, G. G.; Struchkov, Yu. T.; Kalinin, D. I.; Neigauz, M. G. *Zh. Strukt. Khim.* **1973**, *14*, 852.
- (56) Imahori, H.; El-Khouly, M. E.; Fujitsuka, M.; Ito, O.; Sakata, Y.; Fukuzumi, S. *J. Phys. Chem. A* **2001**, *105*, 325.
- (57) Wiederrecht, G. P.; Svec, W. A.; Wasielowski, M. R.; Galili, T.; Levanon, H. *J. Am. Chem. Soc.* **2000**, *122*, 9715.